

Scanning SQUID microscopy on polycrystalline $\text{SmFeAsO}_{0.85}$ and $\text{NdFeAsO}_{0.94}\text{F}_{0.06}$

CLIFFORD W. HICKS¹, THOMAS M. LIPPMAN¹, KATHRYN A. MOLER^{1*}, MARTIN E. HUBER², ZHI-AN REN³,
ZHONG-XIAN ZHAO³

¹*Geballe Laboratory for Advanced Materials, Stanford University, Stanford, California, 94305, USA*

²*Departments of Physics and Electrical Engineering, University of Colorado at Denver, Denver, Colorado, 80217-3364, USA*

³*National Laboratory for Superconductivity, Institute of Physics and Beijing National Laboratory for Condensed Matter Physics, Chinese Academy of Sciences, P.O. Box 603, Beijing 100190, P.R. China*

(Received August 15, 2008)

The order parameter of the recently-discovered ferric arsenide family of superconductors remains uncertain. Some early experiments on polycrystalline samples suggested line nodes in the order parameter, however later experiments on single crystals have strongly supported fully-gapped superconductivity. An absence of nodes does not rule out unconventional order: π phase shifts between the separate Fermi sheets and time-reversal symmetry-breaking components in the order parameter remain possibilities. One test for unconventional order is scanning magnetic microscopy on well-coupled polycrystalline samples: d - or p -wave order would result in orbital frustration, leading to spontaneous currents and magnetization in the superconducting state. We have performed scanning SQUID microscopy on $\text{SmFeAsO}_{0.85}$ and $\text{NdFeAsO}_{0.94}\text{F}_{0.06}$, and in neither material do we find spontaneous orbital currents, ruling out p - or d -wave order.

KEYWORDS: ferro-oxypnictide, pnictide, scanning SQUID microscopy, order parameter, penetration depth, NdFeAsO , SmFeAsO

The ferric arsenide families of superconductors $\text{LnFeAsO}_{1-x}\text{F}_y$, where Ln is a lanthanide, and $(\text{A,K})\text{Fe}_2\text{As}_2$, $\text{A} = \text{Ca, Sr, or Ba}$, show a cuprate-like phase diagram with magnetic order in the parent compounds that is suppressed and replaced with superconducting order with increasing doping. Whether magnetic fluctuations are involved in the pairing is an open question. A vital clue to the pairing interaction would be to know the superconducting order parameter (OP).

Proposals for the OP include s order, both with^{1,2)} and without³⁾ a π phase shift between the central hole Fermi sheet and outer electron sheets; $d_{x^2-y^2}$, both with⁴⁾ and without¹⁾ nodes on the electron sheets; p ⁵⁾ and $s + d$ ⁶⁾ order.

Angle-resolved photoemission (ARPES) experiments have resolved a superconducting gap in single crystals of $\text{Ba}_{0.6}\text{K}_{0.4}\text{Fe}_2\text{As}_2$ ^{7,8)} and $\text{NdFeAsO}_{0.90}\text{F}_{0.10}$.⁹⁾ On the hole Fermi sheets (centered on the Γ point) the gap is observed to be isotropic or nearly isotropic, suggesting s order; pure p or d orders would require a time-reversal symmetry-breaking (TRSB) component to lift the nodes on the hole sheets. The low-temperature penetration depth variation of single crystals of $\text{SmFeAsO}_{0.85}\text{F}_{0.15}$ ¹⁰⁾ and $\text{NdFeAsO}_{0.90}\text{F}_{0.10}$ ¹¹⁾ has been measured by RF tunnel diode resonators and also found to be consistent with fully-gapped superconductivity. Point contact measurements on polycrystalline $\text{SmFeAsO}_{1-x}\text{F}_x$ have suggested both nodal¹²⁾ and nodeless¹³⁾ superconductivity.

These experiments are not phase-sensitive, however. Scanning magnetic microscopy of polycrystalline samples is a phase-sensitive technique: if the OP is unconventional there may be an intrinsic phase shift between tunneling into adjacent faces of a grain, *e.g.* a π shift between tunneling in the [100] and [010] directions in a $d_{x^2-y^2}$ su-

perconductor. If, on going around a loop passing through more than one grain, the net phase shift is not a multiple of 2π , a spontaneous orbital current will emerge in the superconducting state. This has been demonstrated by the observation of half-integral flux quanta in tricrystal cuprate samples¹⁴⁾ and complex patterns of magnetization in polycrystalline cuprate samples.¹⁵⁾

p and d orders, with or without TRSB components, would definitely result in orbital frustration in polycrystalline samples. For s order to result in frustration there would need to be a π shift between the hole and electron sheets, and different sheets would have to dominate a and c axis tunneling.

In earlier work we performed scanning SQUID microscopy on a well-coupled polycrystalline $\text{NdFeAsO}_{0.94}\text{F}_{0.06}$ sample and did not find spontaneous orbital currents.¹⁶⁾ Here we extend this technique to a polycrystalline $\text{SmFeAsO}_{0.85}$ sample. Compared with the $\text{NdFeAsO}_{0.94}\text{F}_{0.06}$ sample the grains are larger. The bulk critical current is higher, indicating better intergrain coupling. Also, by better alignment of the SQUID to the sample we were able to scan closer to the surface. All of these would make spontaneous moments more visible.

The $\text{SmFeAsO}_{1-\delta}$ sample, of nominal oxygen content 0.85, was grown by a high-pressure technique and has an onset T_c of 54 K. The grains are well-coupled: we resolve individual vortices at temperatures up to 52 K, and magneto-optical imaging and remanent magnetization measurements on a sample from the same batch indicate a bulk critical current of $\approx 4000 \text{ A/cm}^2$ at 5 K.¹⁷⁾ We polished the sample to a shiny surface using Al_2O_3 polishing paper, without any lubricant.

Our SQUID is a niobium-based scanning susceptometer design.¹⁸⁾ Figure 1(a) is an image of the front end of the SQUID. Magnetic flux is coupled into the $4.6 \mu\text{m}$

*E-mail: kmoler@stanford.edu

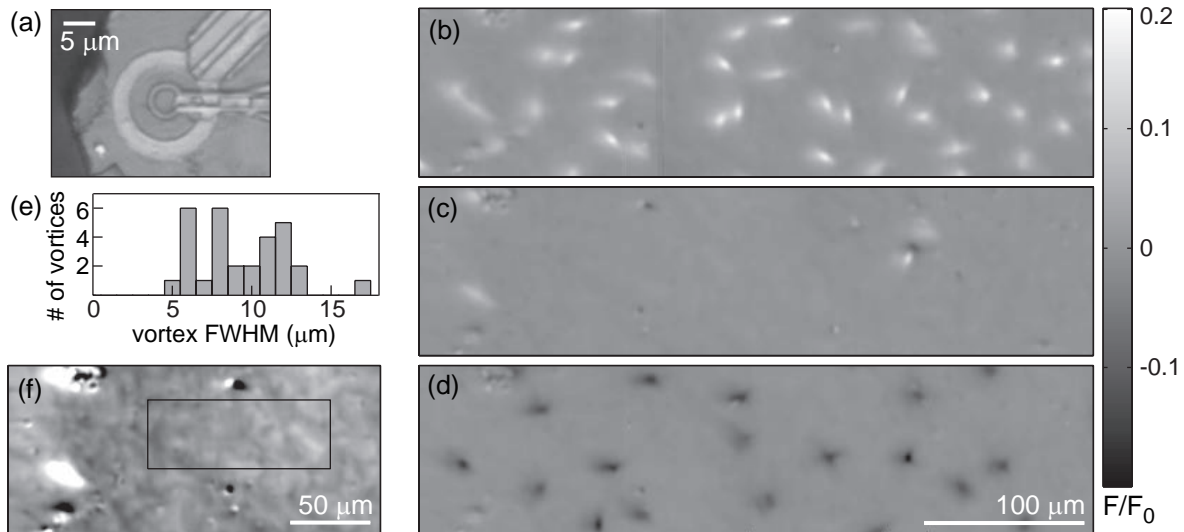


Fig. 1. (a) Image of the front end of the SQUID; the pick-up coil is the inner loop and the field coil the outer loop. (b-d) Scans of a the same area of polycrystalline sample of SmFeAsO_{0.85} in different fields. Each image is on the same length and color scales. $T = 4.4$ K. Applied field during cooling and scanning: (b) 33 mG, (c) 17.4 mG, and (d) 8.4 mG. (There appears to be a ≈ -17 mG background field.) (e) Histogram of the observed vortex FWHMs for the vortices in panel (d); two FWHMs are plotted per vortex. (f) A section of panel (c) on an expanded color scale; the grayscale spans 50 $m\Phi_0$. The area indicated is used to analyze the background.

diameter pick-up coil (the inner coil), the leads to which are shielded; a signal of $1 \Phi_0 = hc/2e = 20.7 \text{ G}\cdot\mu\text{m}^2$ corresponds to a mean B_z in the pick-up coil of ≈ 1.25 G. The larger loop around the pick-up coil is a field coil; a measure of the local susceptibility can be obtained by applying a local field with this coil and measuring the response in the pick-up coil.

Figure 1(b-d) show scans of SmFeAsO_{0.85} at 4.4 K, cooled in different fields. Individual vortices are clearly resolved. They can be cancelled by cooling in an applied field, and most appear in different places after thermal cycling in different fields. All the vortices in Fig. 1(d) integrate to within 20% of Φ_0 , a level of error accounted for by uncertainty in the background. These observations indicate that these are Φ_0 vortices, rather than frustration-related spontaneous moments.

In addition to the vortices a few prominent magnetic dipoles and a widespread irregular background are visible, shown in Fig. 1(f). By lifting the SQUID to just above the sample, the sample temperature can be raised while maintaining the SQUID below its T_c . The dipoles persist above T_c while the irregular background disappears at T_c . In the area indicated in Fig. 1(f) the root-mean-square signal, after subtraction of a second-order polynomial background, is $4.3 m\Phi_0$. On eight different thermal cycles, with the cooling field varied between 8.7 and 33 mG, this background was identical to the extent visible between vortices. Therefore it is not due to spontaneous orbital currents, which result in moments polarizable by an external field.^{15,19} The most likely source of the background is an uncanceled in-plane field: we must apply ≈ 17 mG to cancel the local z -axis field, so an in-plane field of similar magnitude can be expected. This would result in in-plane vortices which would leak out near the surface, and also in-plane field lines above the sample that would deflect upward and downward on

passing over the inhomogeneous surface, resulting in a mottled background signal.

Figure 1(e) shows the distribution of the observed full-width half-maxima of the vortices in Fig. 1(d). The minimum observed FWHMs are $\approx 6 \mu\text{m}$, indicating the resolution limit. Far above an isotropic, homogeneous superconductor the field of a vortex approaches that of a monopole source placed one penetration depth, λ , beneath the surface. In this model, observation of a FWHM of $6 \mu\text{m}$ with a $4.6 \mu\text{m}$ pick-up coil indicates an effective scan height, the actual scan height plus λ , of $\approx 3 \mu\text{m}$.

Most of the vortices have irregular shapes, and many of the observed FWHMs exceed $6 \mu\text{m}$ by a significant margin, indicating that the vortices in the sample are spread out on the range of microns. Many of the vortices are elongated, resolution-limited along one axis and $\sim 10 \mu\text{m}$ wide along the other, suggesting Josephson vortices trapped in junctions between grains.

A susceptibility scan (Fig. 2(a)) shows clearly the granular nature of the sample. Over strongly superconducting areas the field coil is partially shielded by the Meissner screening of the sample, and the coupling between the pick-up coil flux and the field coil current is reduced. For this SQUID the coupling in vacuum is $0.83 \Phi_0/\text{mA}$. Over this sample the minimum observed coupling was $0.44 \Phi_0/\text{mA}$, and the peak of the distribution $0.57 \Phi_0/\text{mA}$. The field coil can be approximated as a thin wire whose diameter is the inner diameter of the actual coil ($11.7 \mu\text{m}$); a coupling of 0.44 – $0.57 \Phi_0/\text{mA}$ indicates an effective scan height of 3 – $4.5 \mu\text{m}$ (that is, 3 – $4.5 \mu\text{m}$ above a theoretical $\lambda = 0$ plane).

An electron backscatter diffraction (EBSD) image, a technique which reveals grain orientation, of a sample from the same batch is shown in Fig. 2(b). In a circle approximation the grains average 8 – $9 \mu\text{m}$ in diameter. A d - or p -wave OP would give well-defined spontaneous

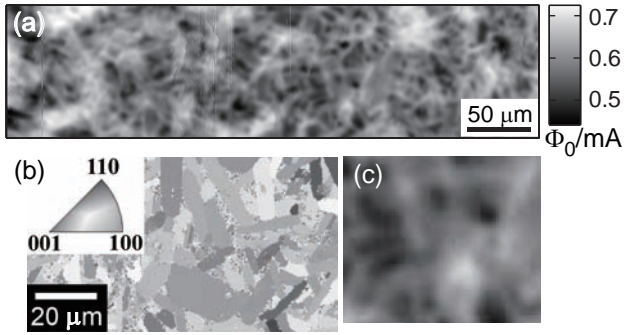


Fig. 2. (a) Susceptibility scan of SmFeAsO_{0.85} at $T = 4.4$ K. (b) EBSD scan of a different SmFeAsO_{0.85} sample from the same batch. (c) For comparison, a section of (a) on the same length scale as (b).

moments if the typical intergrain Josephson penetration depth, λ_J , is comparable to or smaller than the typical grain boundary length. This condition appears to be satisfied, and p and d order ruled out.

For confirmation, we estimate λ_J .

$$\lambda_J = \left(\frac{\hbar c^2}{8\pi e d j_C} \right)^{1/2}, \quad (1)$$

where d is the magnetic width of the junction and j_C its critical current density. $d = d_0 + \lambda_1 + \lambda_2$, where d_0 is the actual intergrain spacing and λ_1 and λ_2 are the penetration depths of the two grains, which will fall somewhere between λ_{ab} and λ_c . Taking $d \sim 2 \mu\text{m}$, $j_C \sim 4000 \text{ A/cm}^2$ gives $\lambda_J \sim 2 \mu\text{m}$.

The observed vortex widths and effective scan height, h , together give another empirical estimate of λ_J . The form of Josephson vortices in a 1-D junction is obtained by solution of a sine-Gordon equation,

$$\frac{\partial^2 \phi}{\partial x^2} = \frac{1}{\lambda_J^2} \sin(\phi(x) + \theta(x)). \quad (2)$$

where $\phi(x)$ is the phase difference between the two grains at position x along the junction and $\theta(x)$ is a frustration phase (set to zero everywhere for solving for a Josephson vortex). We extend the solution obtained from this equation to above the sample by modeling it as a line of monopole sources a distance h beneath the SQUID, then obtain the expected signal by integrating the z component of the resulting field over the pick-up coil area. At $h = 3\text{--}4.5 \mu\text{m}$, an observed FWHM of $12 \mu\text{m}$ yields $\lambda_J = 2.5\text{--}3.2 \mu\text{m}$.

The applicability of the sine-Gordon equation to this case is approximate: $\lambda_J \sim d$, so we are not in the narrow junction limit. However it provides a useful estimate of the expected signal from orbital frustration. Using the method described in refs. 20 and 16, we simulate a long junction divided into domains. In each domain $\theta(x)$ is set to π with probability P , and zero otherwise. The result is again taken as a line of monopole sources. We set $h = 4 \mu\text{m}$, mean domain length = $3 \mu\text{m}$ and $P = 0.25$. With $\lambda_J = 3, 3.75$ and $4.5 \mu\text{m}$, rms expected signals of 11.3, 8.3 and $6.2 \text{ m}\Phi_0$ are obtained, respectively, all comparable to the $4.3 \text{ m}\Phi_0$ background. Therefore it is very unlikely

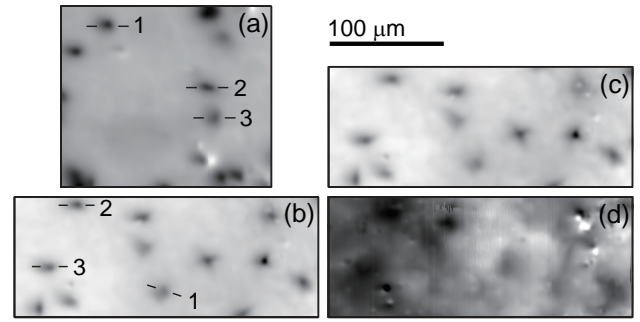


Fig. 3. (a) Scanning SQUID image of NdFeAsO_{0.94}F_{0.06} at 7.5K. The grayscale spans $0.159 \Phi_0$. (b–d): SmFeAsO_{0.85} at 6, 44 and 52 K, respectively. The grayscale spans 0.173, 0.142 and $0.030 \Phi_0$. The numbers indicate sections in Fig. 4, and all images are on the length scale indicated above (c).

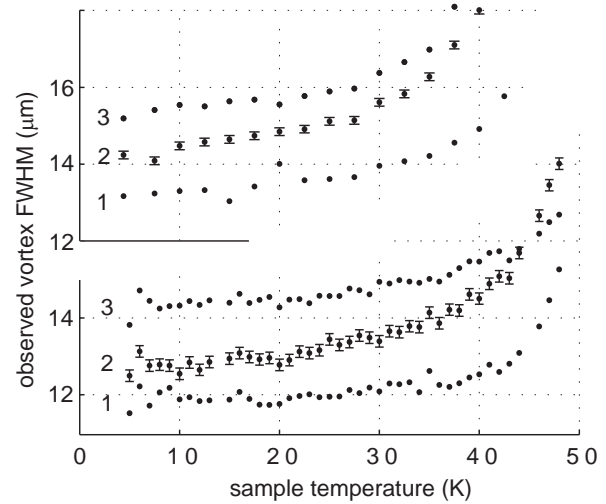


Fig. 4. Top: observed vortex FWHMs in NdFeAsO_{0.94}F_{0.06}, and bottom: in SmFeAsO_{0.85}. The numbers correspond to the sections indicated in Fig. 3. The error bars are estimated from the known error in the scan height; the scan height affects all features in a given scan so errors are correlated.

that the background is obscuring an orbital frustration signal.

A few scans of SmFeAsO_{0.85} and NdFeAsO_{0.94}F_{0.06} at elevated temperatures are shown in Fig. 3. To track changes in the vortex FWHMs, we subtract a polynomial background fit to the areas between vortices and perform cubic spline interpolations to sections through vortex centers. Heating the sample also heats the piezoelectric elements of the scanner slightly; we correct for variation in the elements by tracking the distances between vortices. The results are shown in Fig. 4. For both compounds the vortex widths saturate, within our resolution, for $T < 20$ K, consistent with fully-gapped superconductivity.

In conclusion, scanning SQUID microscopy on polycrystalline samples of SmFeAsO_{0.85} show an absence

of spontaneous orbital currents in the superconducting state. While our experiment cannot definitively distinguish π -shifted and non- π -shifted s orders, it does rule out pure p - and d -wave order parameters.

This project was supported by the U.S. Department of Energy (DE-AC02-76SF00515). We thank David Larbalestier, Alex Gurevich, and Doug Scalapino for useful discussion. We also thank Fumitake Kametani and David Larbalestier for providing the EBSD image.

- 1) K. Kuroki, S. Onari, R. Arita, H. Usui, Y. Tanaka, H. Kontani and H. Aoki: Phys. Rev. Lett. **101** (2008) 087004.
- 2) I.I. Mazin, D.J. Singh, M.D. Johannes and M.H. Du: Phys. Rev. Lett. **101** (2008) 057003.
- 3) Fa Wang, Hui Zhai, Ying Ran, A. Vishwanath and D.H. Lee: cond-mat/08070498.
- 4) Z.J. Yao, J.X. Li and Z.D. Wang: cond-mat/08044166.
- 5) P.A. Lee and X.G. Wen: cond-mat/08041739.
- 6) K. Seo, B.A. Bernevig and Jiangping Hu: cond-mat/08052958.
- 7) H. Ding, P. Richard, K. Nakayama, T. Sugawara, T. Arakane, Y. Sekiba, A. Takayama, S. Souma, T. Sato, T. Takahashi, Z. Wang, X. Dai, Z. Fang, G.F. Chen, J.L. Luo and N.L. Wang: cond-mat/08070419.
- 8) Lin Zhao, H.Y. Liu, W.T. Zhang, J.Q. Meng, X.W. Jia, G.D. Liu, X.L. Dong, G.F. Chen, J.L. Luo, N.L. Wang, Wei Lu, G.L. Wang, Yong Zhou, Yong Zhu, X.Y. Wang, Z.X. Zhao, Z.Y. Xu, C.T. Chen and X.J. Zhou: cond-mat/08070398.
- 9) T. Kondo, A.F. Santander-Syro, O. Copie, Chang Liu, M.E. Tillman, E.D. Mun, J. Schmalian, S.L. Bud'ko, M.A. Tanatar, P.C. Canfield and A. Kaminski: cond-mat/08070815.
- 10) L. Malone, J.D. Fletcher, A. Serafin, A. Carrington, N.D. Zhigadlo, Z. Bukowski, S. Katrych and J. Karpinski: cond-mat/08063908.
- 11) C. Martin, R.T. Gordon, M.A. Tanatar, M.D. Vannette, M.E. Tillman, E.D. Mun, P.C. Canfield, V.G. Kogan, G.D. Samolyuk, J. Schmalian and R. Prozorov: cond-mat/08070876.
- 12) Y.L. Wang, Lei Fang, Peng Cheng, Cong Ren and H.H. Wen: cond-mat/08061986.
- 13) T.Y. Chen, Z. Tesanovic, R.H. Liu, X.H. Chen and C.L. Chien: Nature **453** (2008) 1224.
- 14) C.C. Tsuei, J.R. Kirtley, C.C. Chi, Lock See Yu-Jahnes, A. Gupta, T. Shaw, J.Z. Sun and M.B. Ketchen: Phys. Rev. Lett. **73** (1994) 593.
- 15) J.R. Kirtley, A.C. Mota, M. Sigrist and T.M. Rice: J. Phys.: Condens. Matter **10** (1998) L97.
- 16) C.W. Hicks, T.M. Lippman, K.A. Moler, M.E. Huber, Z.A. Ren and Z.X. Zhao: cond-mat/08070467.
- 17) A. Yamamoto, A.A. Polyanskii, J. Jiang, F. Kametani, C. Tarantini, F. Hunte, J. Jaroszynski, E.E. Hellstrom, P.J. Lee, A. Gurevich, D.C. Larbalestier, Z.A. Ren, J. Yang, X.L. Dong, W. Lu and Z.X. Zhao: Supercond. Sci. Technol. **21** (2008) 095008.
- 18) M.E. Huber, N.C. Koshnick, H. Bluhm, L.J. Archuleta, T. Azua, P.G. Björnsson, B.W. Gardner, S.T. Halloran, E.A. Lucero and K.A. Moler: Rev. Sci. Instrum. **79** (2008) 053704.
- 19) M. Sigrist and T.M. Rice: Rev. Mod. Phys. **67** (1995) 503.
- 20) J.R. Kirtley, K.A. Moler and D.J. Scalapino: Phys. Rev. B **56** (1997) 886.